

Electronic Supplementary Information

Towards efficient electrocatalyst for oxygen reduction by doping cobalt into graphene-supported graphitic carbon nitride

Shaohong Liu, Yanfeng Dong, Zhiyu Wang, Huawei Huang, Zongbin Zhao, and Jieshan Qiu**

*Carbon Research Laboratory, Liaoning Key Lab for Energy Materials and Chemical Engineering,
State Key Lab of Fine Chemicals, Dalian University of Technology,
Dalian 116024, P. R. China*

**Corresponding author: E-mail: zywang@dlut.edu.cn (Z. Wang); jqiu@dlut.edu.cn (J. Qiu)*

Experimental Details

Materials synthesis: Graphite oxide (GO) was prepared via a modified Hummers' method reported elsewhere. The Pcy@G nanosheets were synthesized by refluxing the mixture of cyanamide (5 mL, 50 wt.%, Aladdin) and GO suspension (50 mL, 0.5 mg mL⁻¹) at 90 °C for 24 h (Pcy refers to the polymer of cyanamide). Pcy was prepared by the same procedure in the absence of GO.

For the synthesis of Co-C₃N₄@G nanocomposites, the above Pcy@G nanosheets was dispersed in 50 mL of 0.03 M Co(OAc)₂ ethanolic solution under ultrasonic for 15 min. After stirred for 12h, the product was harvested by several centrifugation-rinse cycles, followed by annealing at 550 °C for 4 h in N₂. For comparison, C₃N₄@G nanocomposites were also prepared by the same procedure in the absence of Co(OAc)₂.

For the synthesis of C₃N₄@G, the above Pcy was mechanically mixed with GO (25 mg) followed by annealing at 550 °C for 4 h in N₂. C₃N₄ and G nanosheets were prepared by the same procedure in the absence of GO and Pcy, respectively.

Material characterization: The morphology of the samples was characterized with field-emission scanning electron microscopy (FESEM, FEI NanoSEM 450) and transmission electron microscopy (TEM, Tecnai G220). Powder X-ray diffraction (XRD) patterns were recorded on a Rigaku D/Max

2400 type X-ray spectrometer with Cu K α radiation ($\lambda = 1.5406 \text{ \AA}$). The surface characteristics of the samples were investigated using a Bruker Equinox 55 Fourier transform infrared spectrometer (FTIR) and Thermo ESCALAB 250 X-ray photoelectron spectrometer (XPS). The textural properties of the samples were measured by Micrometrics ASAP 2020 Surface Area and Porosity Analyzer at 77 K.

Electrochemical measurement: The measurement of oxygen reduction reaction (ORR) was performed using a CHI 760D electrochemical workstation with a three-electrode system in KOH solution (100 mL, 0.1 M). A glassy-carbon (GC) rotating disk electrode (RDE) ($d = 5 \text{ mm}$) was used as working electrode while a Pt wire and an Ag/AgCl electrode saturated with KCl solution was employed as counter and reference electrode, respectively. Before the measurement, the electrolyte was bubbled with O₂ or Ar flow for 30 min. A gas flow was maintained over the electrolyte during the measurement to ensure continuous gas saturation. For the test, 2 mg of the samples (e.g., Co-C₃N₄@G, C₃N₄@G, or commercial JM Pt/C 20 wt.%) were ultrasonically dispersed in ethanol (1 mL) to form a uniform suspension. A part of the catalyst ink (10 μL) was then loaded onto a GC electrode by microsyringe with ethanol solution of Nafion (5 μL , 0.1 wt.%) as the binder, yielding a mass loading of 0.1 mg cm⁻². For CV and RDE measurements, the working electrodes were scanned between -1.0 V to 0.2 V at a scan rate of 10 mV s⁻¹ at room temperature under continuous O₂ or Ar flow. RDE measurements were conducted at different rotating rate from 400 to 2000 rpm. Methanol tolerance of the catalyst was tested by conducting the ORR in presence of methanol (14 mL, 3 M) in O₂-saturated KOH solution (100 mL, 0.1 M) by the similar procedure. In Tafel plot, the kinetic current was calculated from the mass-transport correction of RDE data by a formula of $J_K = (J^*J_L) / (J_L - J)$.

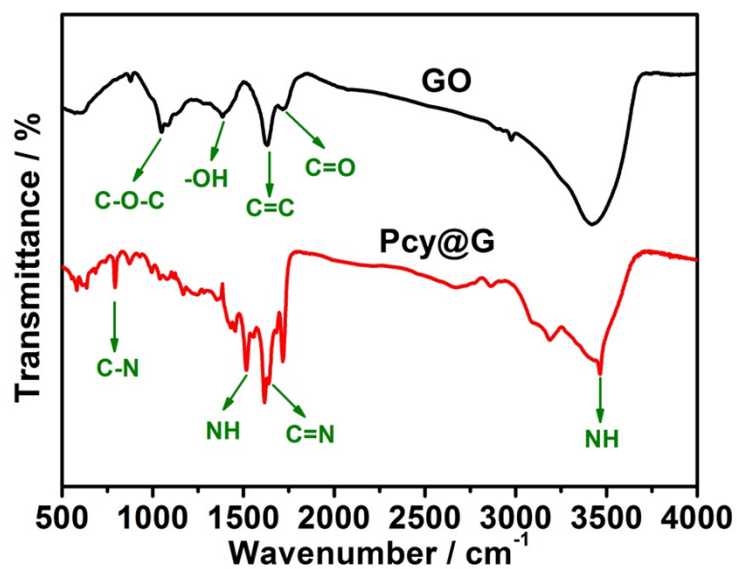


Fig. S1 FTIR spectra of GO and Pcy@G nanocomposites.

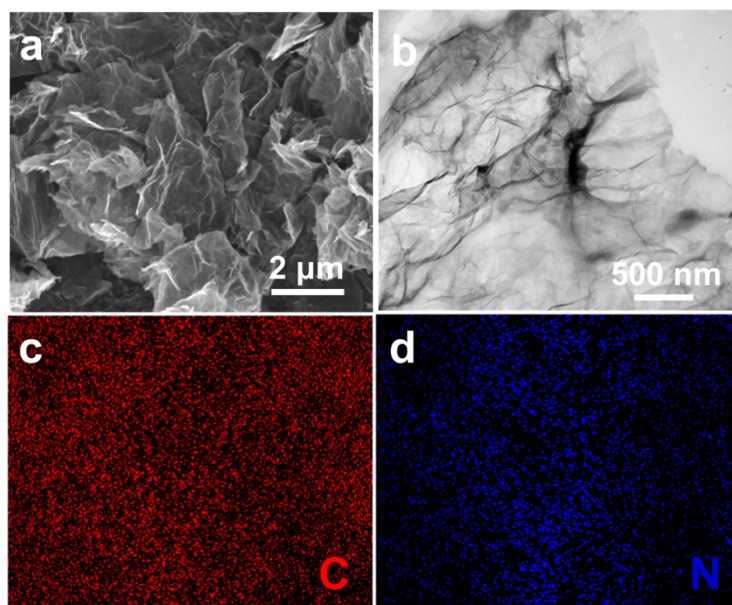


Fig. S2 (a) SEM and (d) TEM images of Pcy@G nanocomposites; (c and d) elemental mapping showing the uniform distribution of carbon and nitrogen element in Pcy@G nanocomposites.

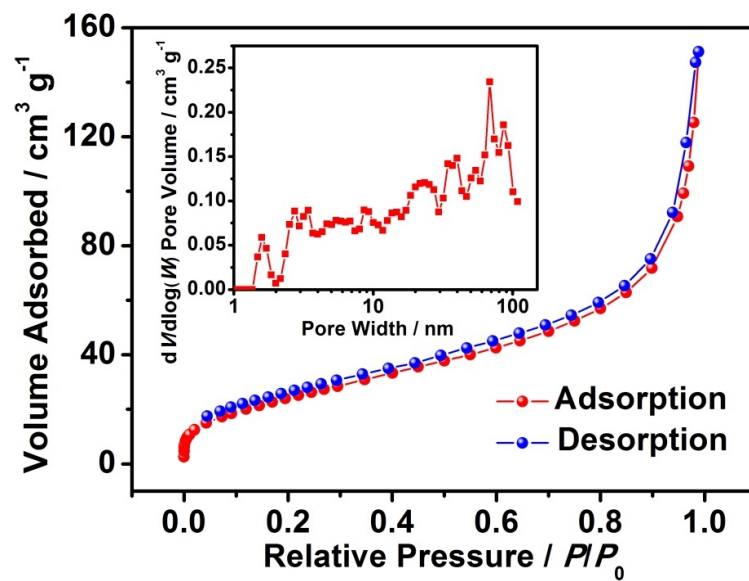


Fig. S3 N₂ adsorption-desorption isotherm of Co-C₃N₄@G sample. The inset is corresponding pore size distribution.

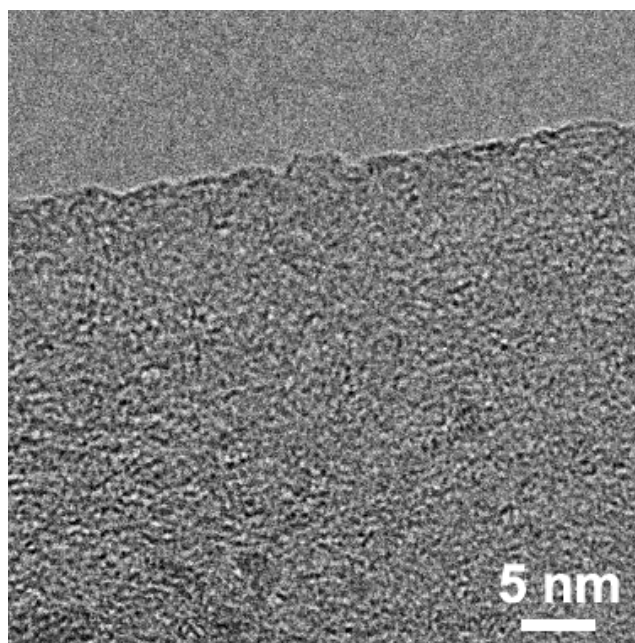


Fig. S4 HRTEM image of Co-C₃N₄@G sample.

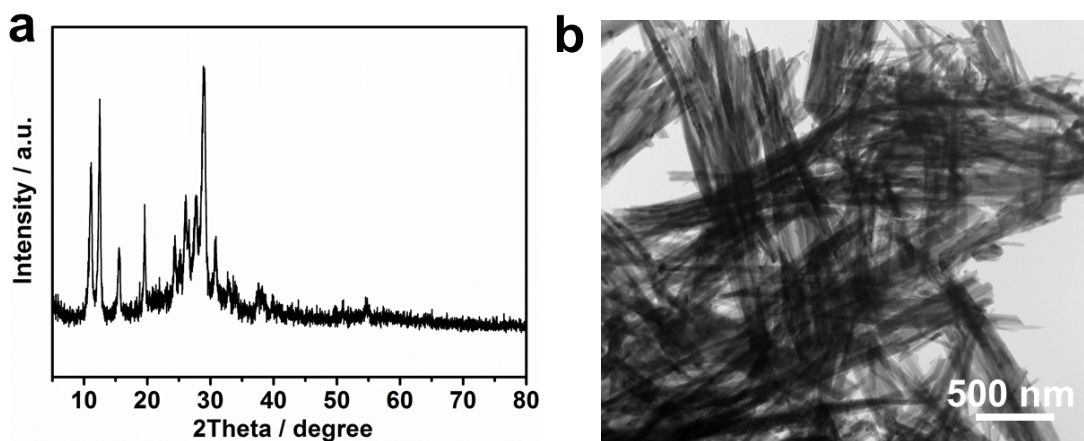


Fig. S5 (a) XRD pattern and (b) TEM image of Pcy.

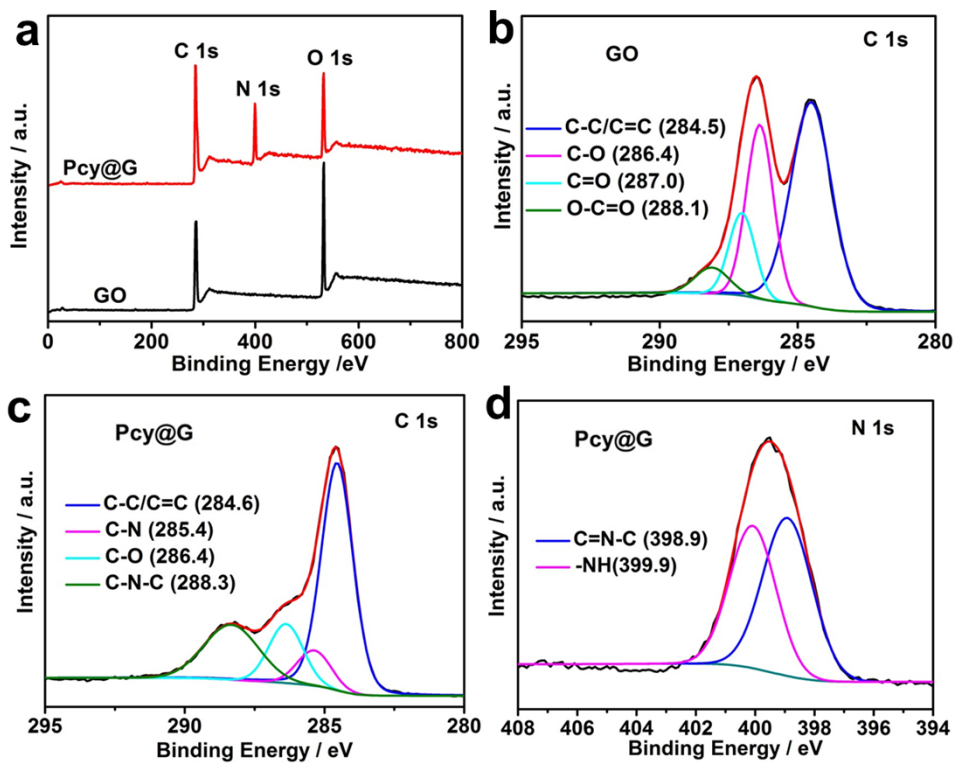


Fig. S6 (a) Full XPS survey scan of GO and Pcy@G nanocomposites; (b) high-resolution C 1s spectrum of GO; (c and d) high-resolution C 1s and N 1s spectrum of Pcy@G nanocomposites, respectively.

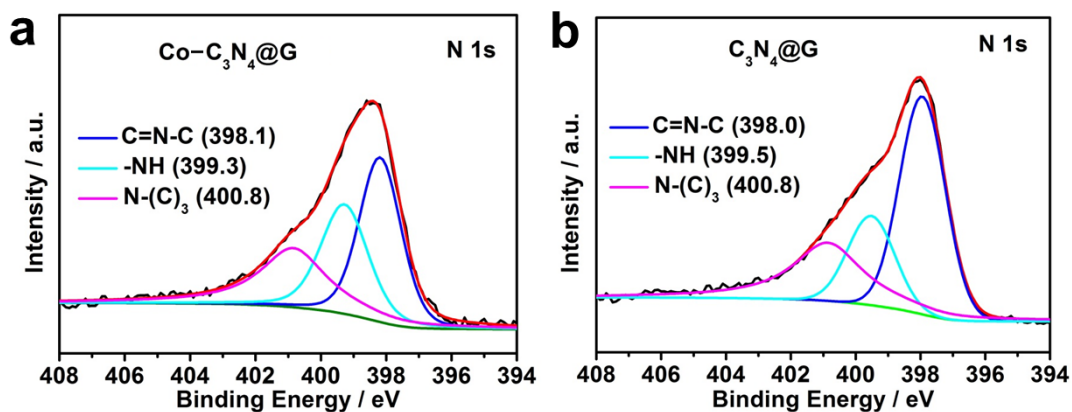


Fig. S7 High-resolution N 1s spectrum of (a) Co-C₃N₄@G and (b) C₃N₄@G nanocomposites.

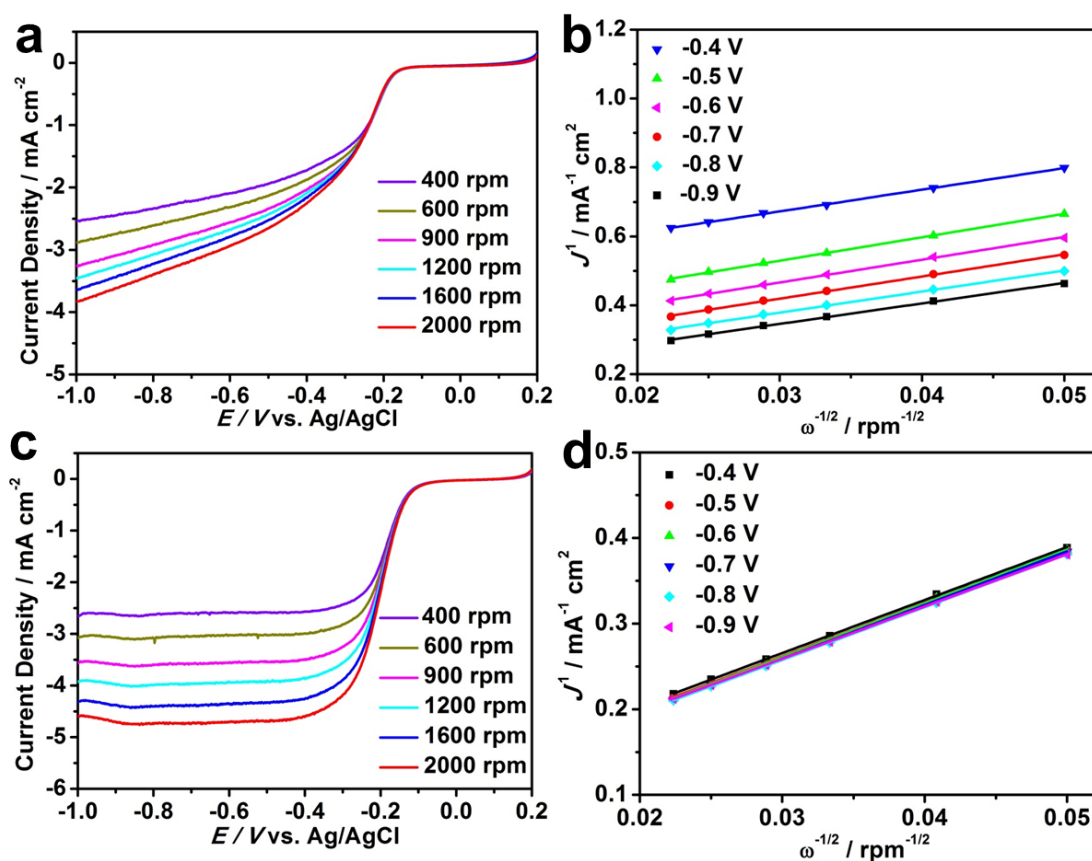


Fig. S8 LSVs of (a) C₃N₄@G and (c) Pt/C electrodes in O₂-saturated 0.1 M KOH solution at different rotation rates with a scan rate of 10 mV s⁻¹; Koutecky-Levich plots for (b) C₃N₄@G and (d) Pt/C electrodes at various potentials.

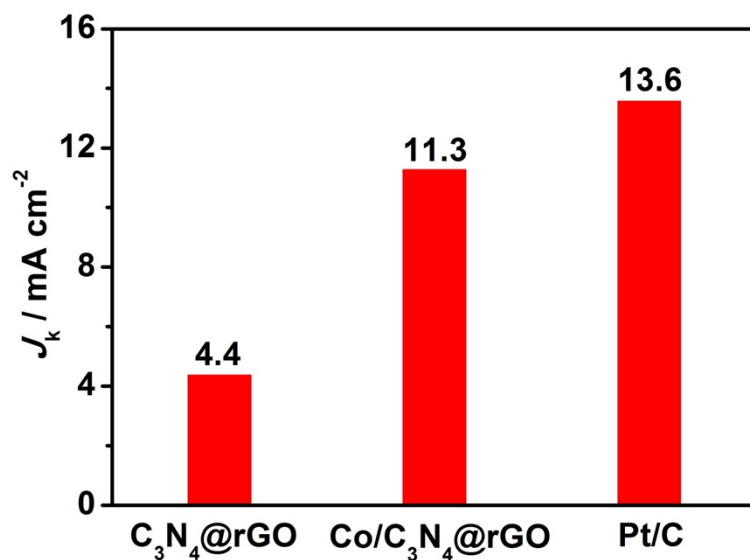


Fig. S9 The calculated kinetic-limiting current densities of $\text{C}_3\text{N}_4@\text{G}$, $\text{Co-C}_3\text{N}_4@\text{G}$, and Pt/C electrodes at -0.7 V.

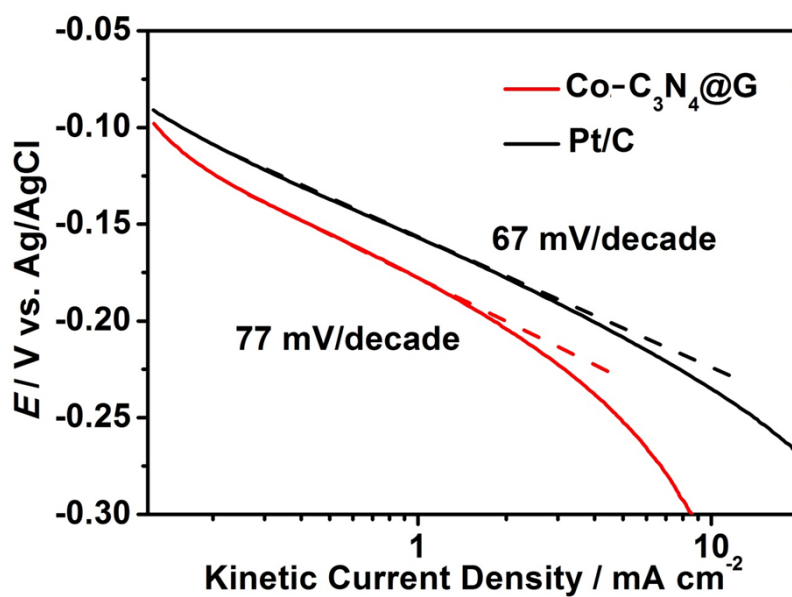


Fig. S10 Tafel plots of $\text{Co-C}_3\text{N}_4@\text{G}$ and Pt/C electrodes obtained from the LSV curves at a rotation rate of 1600 rpm.

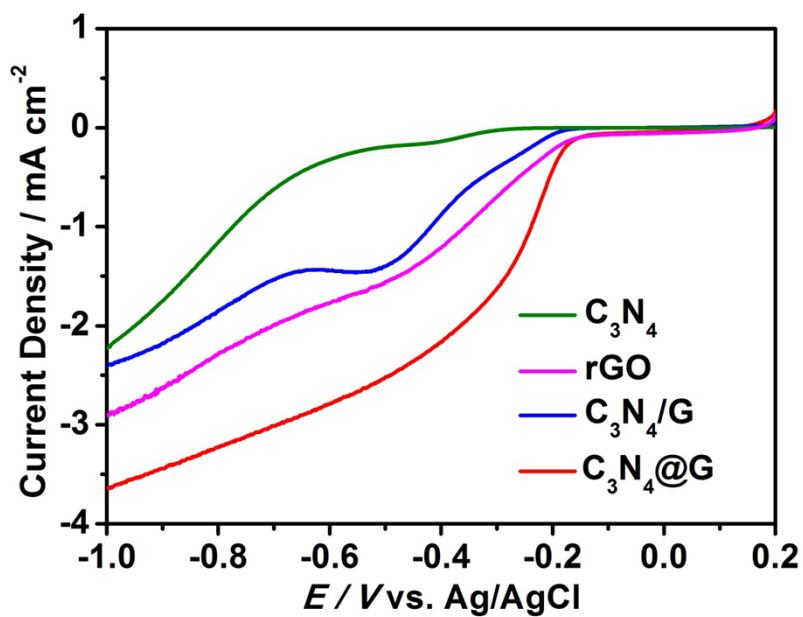


Fig. S11 LSVs of C_3N_4 , G, C_3N_4/G and $C_3N_4@G$ electrodes in O_2 -saturated 0.1 M KOH solution at a rotation rate of 1600 rpm with a scan rate of 10 mV s^{-1} .

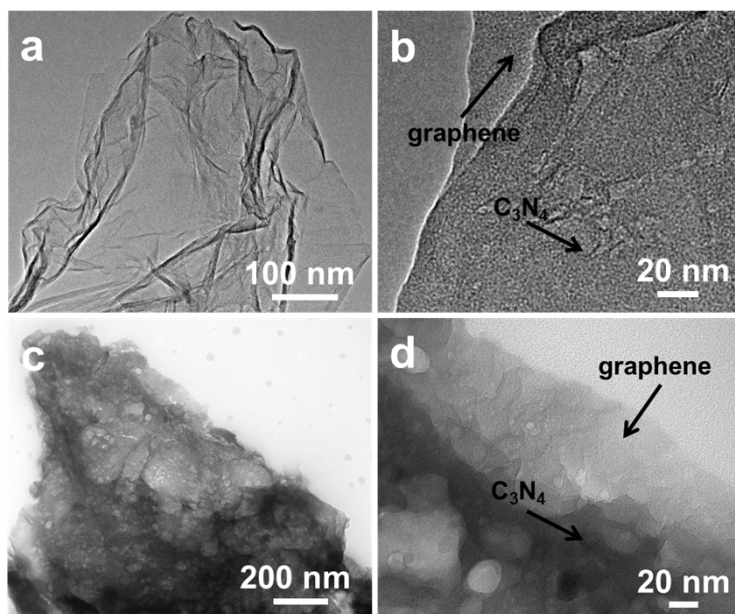


Fig. S12 TEM images of (a and b) $C_3N_4@G$ and (c and d) C_3N_4/G nanocomposites.